

Research Journal of Pharmaceutical, Biological and Chemical Sciences

Genotoxicity and Ultrastructural Studies of the Effect of Cisplatin on the Cortex of Kidney of Albino Male Mice.

Cecil A Matta¹, Azza A Attia², and Hanan A Khaliffa³.

^{1,2}Zoology Department, Faculty of Scienc, Alexandria University, Egypt.

³Faculty of Scienc, Omar Elmokhtar University, Lybea.

ABSTRACT

Cisplatin is still a frequently used chemotherapeutic agent, despite of its frequent adverse effects, including nephrotoxicity. The present work was done to investigate its harmful effects on the tissue kidney of the male mice. Two groups of mice were injected intraperitoneally with 0.5 ml cisplatin at doses of 0.15 and 0.3 mg/kg BW, two times/weak, for four consecutive weeks. The third group animals was injected with 0.5 ml saline solution as a vehicle, and considered as a control. Chromosomal aberrations test, DNA assay and ultrastructural studies in the tissue of kidney were evaluated. The results revealed that, depending on the dose response, there was an increase in the mortality rate and decrease in the body weights of experimental mice treated with the two dose levels of cisplatin. The chromosomal aberrations include deletion, centric fusion and stickiness, indicating the positive clastogenic effect of cisplatin. Severe DNA damage was more prominent in the tissue kidney of mice administered with 0.3 mg/kg BW cisplatin. Histologically, cisplatin caused severe structural alterations including destruction in the renal tubular cells, and presence of focal hemorrhage in between the tubules. The glomeruli exhibited shrinkage of the glomerular tuft and dilatation in the urinary spaces. At the ultrastructural level, evere atrophy in the glomeruli; rupture of Bowman's capsule and dilatation in the urinary space were observed. At the proximal conpluted tubules, the basal infoldings appeared short and flattened, and large vacuoles were noticed in the cytoplasm. Mostly, the nuclei were pyknotic, the mitochondria were pleomorphic, and there was an increase in the primary and secondary lysosomes. In the distal convoluted tubule cells, the nuclei were mostly pyknotic.

Keywords: Cisplatin, Glomeruli, Genotoxicity, Renal tubules, Chromosomal aberrations, Nephrotoxicity

**Corresponding author*

INTRODUCTION

It is well known that, use of chemotherapy in the treatment of cancer has opened new possibilities for improvement of the quality of life of cancer patients [1]. Chemotherapy involves the use of chemical agents to stop the growth and eliminate cancer cells even at distant sites from the origin of primary tumor. The chemotherapeutic agents can be divided into several categories: Alkylating agents (e.g., cyclophosphamide), antibiotics which affect nucleic acids (e.g., bleomycin), platinum compounds (e.g., cisplatin), mitotic inhibitors (e.g., vincristine), antimetabolites (e.g., 5-fluorouracil), biological response (e.g., interferon), and hormone therapies (e.g., tamoxifen) [2].

Cisplatin [cis-diamminedichloroplatinum] as an efficient platinum-derived alkylating agent is one of the most important chemotherapeutic agents ever introduced. It is used for a wide spectrum in human malignancies [3, 4]. However, its major side effects, nephrotoxicity and hepatotoxicity are the main limiting factors of its clinical use for long term treatment [5]. Miller *et al.* [6] found that the adverse effects of cisplatin could cause nephrotoxicity.

Kidneys are dynamic organs and represent the major control system maintaining the body haemostasis; they are affected by many chemicals and drugs [7]. Ali and Al-Moundhri [8] found that cisplatin could accumulate in the renal tubular cells approximately five times its extracellular concentration. Saad *et al.* [9] indicated that cisplatin induced damage in kidney genomic DNA, lipid peroxidation, inhibition of antioxidant enzymes and alterations of biochemical parameters in plasma and kidney of rats.

After application of cisplatin, damage to DNA may result in DNA fragmentation, chromosomal breaks, and micronucleus formation causing genomic instability, and may lead to mutagenesis, carcinogenesis, or finally to apoptotic cell death [10, 11]. Florea and Büsselberg [12] explained that cisplatin could induce cytotoxicity by interference with transcription and/or DNA replication mechanisms.

Sahu *et al.* [13] indicated that the toxic effects of CP occur through increased oxidative stress and apoptosis. Domitrovic *et al.* [14] found that cisplatin administration resulted in a severe nephropathy, accompanied by impaired histological features of the kidneys. Park *et al.* [15] explained that cisplatin could induce apoptosis via activation of mitochondrial signaling pathways. Custódio *et al.* [16] added that cisplatin causes an increase in the sensitivity of mitochondria to Ca^{2+} -induced mitochondrial permeability transition, interference with mitochondrial bioenergetics by increasing mitochondrial inner membrane permeabilization to H^+ but does not significantly affect H_2O_2 generation by mitochondria. Therefore, the aim of this study was done to evaluate the chromosomal aberration in the bone marrow cells, the extent of DNA damaging in the tissue kidney. Histopathological and ultrastructural changes of the effect of cisplatin on the cortical regions of the kidney of mice were also investigated.

MATERIAL AND METHODS

Material

Animal study

Forty five healthy adult male albino mice were obtained from the Faculty of Agriculture, Alexandria University, Alexandria, Egypt. They were of 3 months old, and weighing 28-32 g each, when the experimentation commenced. All animals were housed in the usual stainless steel cages (5 mice/cage), which were cleaned day by day continuously. They were adapted to the controlled environmental conditions at room temperature of 25 ± 2 °C, and normal photoperiod 12 h/d. Also, they were allowed free access of food (wheat, bread) and drinking water *ad libitum*.

Drug preparation

Cisplatin was purchased from the pharmacy under the international trade name cisplatin MERCK®. It was manufactured by Oncoten Pharma Production GmbH, Rodleben-Germany. Two different dose levels were prepared according to the equivalent prescribed dose for human (5 and 10 mg/Kg body weight) [5, 17], which were calculated to be 0.15 and 0.3 mg/kg BW/mice respectively.

Methods

Treatment

All mice were divided into two experimental groups and one control (each of 14), according to their approximately equal body weights. Two experimental group mice were injected intraperitoneally, two times/week, for 4 consecutive weeks with 0.5 ml of cisplatin at a dose level of 0.15 and 0.3 mg/kg BW. Third group mice was considered as a control and administered with 0.5 ml saline solution (0.9 % NaCl), two times/week, for four consecutive weeks.

Macroscopic examination

During the experiment, all treated mice and the control were carefully examined in order to depict any apparent external changes and/or sign of toxicity. The number of dead mice occurring among them was counted and the percentage of mortality was calculated.

Body weight and weight change

At the end of experiment, the body weight change (%) was estimated by dividing the final body weight / initial body weight $\times 100$.

The chromosomal aberration test

Five mice of each control and the treated mice were used for studying the chromosomal aberrations. According to the method of Preston *et al.* [18], 24 h after administration of the last dose of cisplatin, mice were injected intravenously with 0.5 mg/kg colchicines, 2 h prior to sacrifice. Femurs of each mouse were dissected out quickly, and bone marrow cells were collected by flushing in KCl (0.075 M) and incubated at 37 °C for 25 min. The collected bone marrow cells were centrifuged at 2000 rpm for 10 min, and fixed in acetic acid: methanol (1:3 respectively). Centrifugation and fixation were repeated four times at an interval of 15 min each. The cells were resuspended in a small volume of fixative, dropped onto slides, flame-dried and stained with 5% Giemsa stain for 3-5 min, washed in distilled water to remove excess stain. The best spread metaphase cells were selected, and the structural chromosomal aberrations were scored in 100 metaphases for each animal to a total number of 150 metaphases to obtain the total number of chromosomal aberration.

Histopathological study

At the end of experiment, mice of the experimental groups and the control were dissected out quickly. Small slices of the cortical region of kidney were taken immediately and fixed overnight in a freshly prepared 10% formalin solution. The fixed specimens were processed by the usual recognized histological methods of dehydration, clearing by xylene and embedding in paraffin wax [19]. Serial sections were cut at 5-6 μm thick, stained by hematoxylin-eosin (H&E), examined and photographed by the light microscopy.

Ultrastructural investigation

Very small slices of the cortex of kidney of both control and cisplatin-treated mice were immediately fixed in 2 % OsO_4 , then rinsed in 0.1M phosphate buffer, pH = 7.4 at 4°C for around 1 h, then rinsed in 0.1 M phosphate buffer (pH 7.4). This was followed by post-fixation using 1% buffered OsO_4 (osmium tetroxide) for 1-2 h at 4°C, then the specimens were washed with phosphate buffer for several times for 30 min, dehydrated in ascending grades of ethanol concentration. Tissues were then treated with propylene oxide and embedded in a mixture of 1: 1 of Epon-Araldite. Specimens were embedded in pre-dried gelatine capsule (dried in the oven at 37 °C for 1 h before use). Polymerization was done in the oven at 65 °C for 24 h. Ultrathin sections obtained from such specimens were with a glass knife on LKB ultramicrotome, mounted on 200 mesh naked copper grids, doubled stained with uranyl acetate and lead citrate [20]. Sections were examined by using Jeol 100CX transmission electron microscope at the Faculty of Science, Alexandria University, Alexandria, Egypt.

DNA analysis

According to the method of Saad *et al.* [9], the electrophoretic DNA was assayed for the tissue kidney (five mice of each experimental group and the control).

Statistical analysis

Statistical analysis for all data was done using the SPSS software package version 17.0, and the results were expressed as the mean \pm Standard Error (SE). Then, they were analyzed statistically using one-way analysis of variance (ANOVA). All tests were carried out at a significant level of $P < 0.05$ (P = probability value). Further, analyses of the data were performed with the least significant difference (LSD) to determine which sample was significantly different from control.

RESULTS

External signs of toxicity:

The results revealed that the signs of toxicity were more prominent in mice treated with 0.3 mg/kg bw cisplatin, where fall of body hair and decrease in the body weight were prominent. The mortality rate in mice treated with 0.15 mg/kg BW cisplatin was 15%, increasing to 32.5% in those treated with 0.3 mg/kg BW. Depending on dose response, the body weights of cisplatin-treated mice were significantly decreased ($p \leq 0.05$) versus the control mice (Table 1).

Table 1: % of mortality and body weight change of mice treated with the two doses of cisplatin for four weeks.

Experimental Groups	No. of mice	No. of dead mice	% of mortality	Mean of body weight (g)		% Body weight change
				Initial	Final	
Control mice	40	0	0.0	29.80 \pm 0.76	30.85 \pm 0.17 ^a	3.52 \pm 1.64 ^a
5 mg/kg bw cisplatin	40	6	15.0	28.28 \pm 0.24	26.64 \pm 0.29 ^b	-5.8 \pm 1.29 ^b
10 mg/kg bw cisplatin	40	13	32.5	30.33 \pm 0.22	25.07 \pm 0.28 ^c	-17.34 \pm 0.97 ^c

Data are expressed as mean \pm SE a, b, c: means that there is no significant differences at values of $P \leq 0.05$, among the tested groups when compared to the control.

The chromosomal aberrations

The appearance of chromosomes was studied in the bone marrow metaphase of mitotic division. The chromosome complement of the mouse is composed of $2n = 40$ chromosomes, including 19 pairs of autosomes and a pair of sex chromosome (XX, XY for female and male respectively). All chromosomes are acrocentric (Fig. 1a). Depending on dose response, the results indicated that cisplatin induced various chromosomal aberrations in the bone marrow cells of mice. These aberrations comprised 4 types namely, gaps (0.4%) (Fig. 2a), deletion (0.4%)(Fig. 2b), fragmentation (0.6%) (Fig. 2c), centromeric attenuation (0.2%) (Figs. 2d, 3b). End end to end association in the chromosome is induced by general stickiness oof chromosomes (Figs. 2d). In addition, there was centic fusion (Fig. 3a); ring formation (Fig. 2b, 3a); chromosomal stickiness (Fig. 3c) and Pulverized chromosome at Fig. 3d.

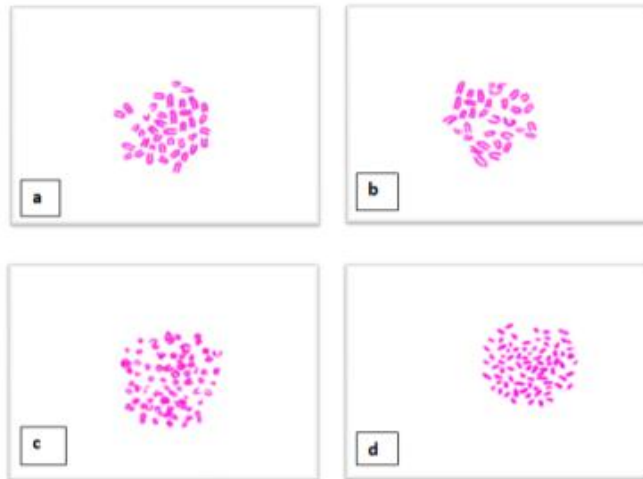


Figure 1: Light micrographs of metaphase of mouse bone marrow cells showing a) Normal acrocentric chromosomes; b) Hypodiploidy; c) polyploidy; d) Endomitosis.

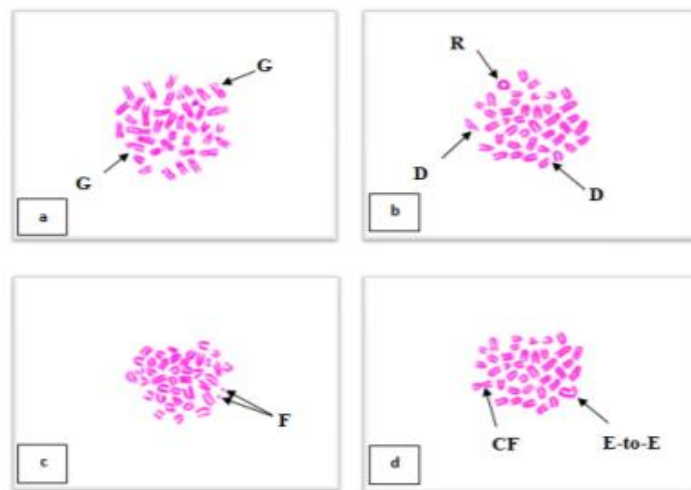


Figure 2: Light micrographs of metaphase chromosomal aberrations of mouse bone marrow cells showing a) gaps (G); b) Ring (R), Deletion (D); c) Fragmentation (F); d) Centric Fusion (CF) end to- end association (E-to-E).

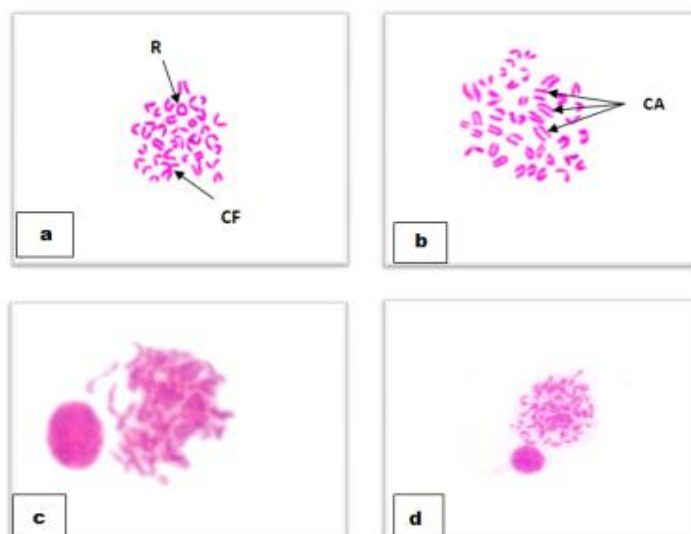


Figure 3: Light micrographs of metaphase chromosomal aberrations of mouse bone marrow cells showing a) Ring (R), centric Fusion (CF); b) Centric attenuation (CA); c) Stickiness; d) Pulverized cells.

DNA assay

The genomic DNA extracted from kidney tissues of the different experimental groups showed that treatment with low-dose cisplatin (0.15 mg/kg BW) caused a partial degradation of genomic DNA characterized only by smearing of DNA fragments (**Fig. 4; Lanes B,C**), compared with the DNA isolated from control samples (**Fig. 4; Lane A**) which showed DNA intact. Whereas, the DNA of high-dose treated mice was evident that administration of cisplatin exhibited dramatic complete degradation of genomic DNA (**Fig. 4; lanes D, E**).

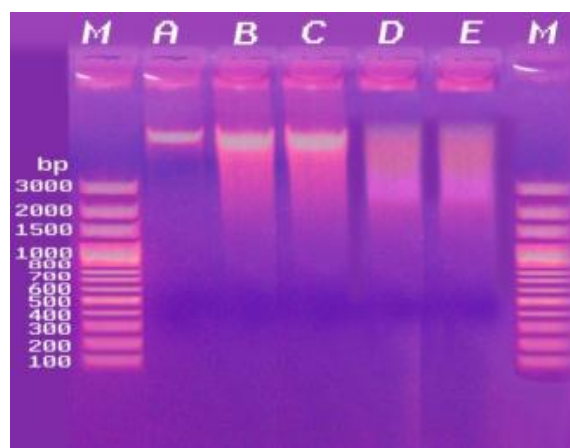


Figure 4: Gel electrophoresis photograph showing the genomic DNA of kidney of control and treated mice. Lane M: DNA marker; Lane A: Control; Lane B, C: 0.15 mg/kg BW cisplatin; Lane D, E: 0.3 mg/kg BW cisplatin.

Histopathological findings

Section in the kidney of control mice is found to divide into an outer dark cortex and an inner light medulla. The renal cortex is composed mainly of millions functional unit (nephrons), each one consists of two major components, the renal corpuscles and the renal tubules. The renal corpuscle consists of a tuft of capillaries, the glomerulus, which is surrounded by a double-walled epithelial capsule called the Bowman's capsule, and the urinary space (Fig. 5).

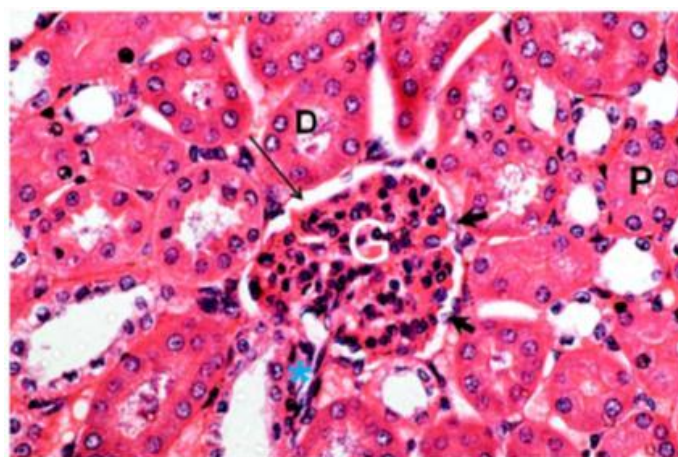


Figure 5: Light micrograph in the renal cortex of control mouse revealing, the glomerulus (G) with distinct urinary space (arrow); notice: the flattened nuclei (arrow head) lining the Bowman's capsule; proximal convoluted tubule (P); distal convoluted tubule (D), X 400.

The proximal convoluted tubules (PCT) possess narrow lumen and their cells have large spherical nuclei, and centrally located prominent nucleoli. The apical surfaces of these cells that face the lumen exhibit abundant microvilli which form the so called brush border (Fig. 6). The distal convoluted tubules (DCT) have wide lumina and bordered by cubical or low columnar epithelial cells, having flattened small nuclei (Fig. 6).

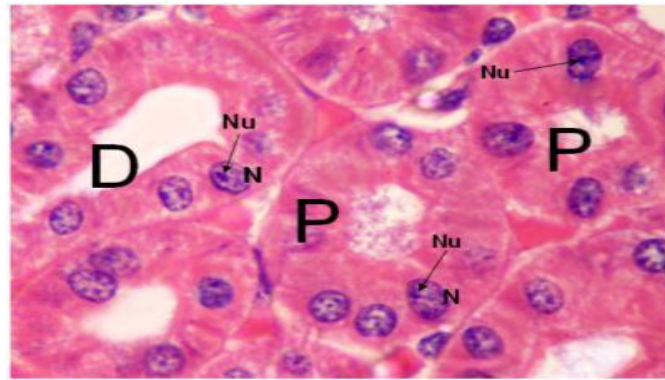


Figure 6: Light micrograph of the renal tubules in kidney of control mouse revealing, proximal convoluted tubules (P) lined by high cuboidal or pyramidal cells, having spherical basally located nuclei (N) and prominent nucleoli (Nu); distal convoluted tubule (D) are lined by cuboidal cells, having rounded-shaped nuclei (N), X 1000.

Ultrastructurally, in the glomerulus, the parietal layer of Bowman's capsule consists of a layer of simple squamous cells which bulges into the urinary space in the region of their nuclei (Fig. 7). The visceral layer of the Bowman's capsule is formed of modified cells called the podocytes which are suspended in the urinary space. These cells are basically stellate with several radiating primary foot processes and secondary processes called the pedicles. These secondary foot processes are in direct contact with the renal filtration barrier, and the ending of these processes interdigitate to cover the glomerular basement membrane and are separated by gaps of uniform width with the "filtration slits" (Figs. 7, 8). The pores, between the pedicles are opened into the urinary space.

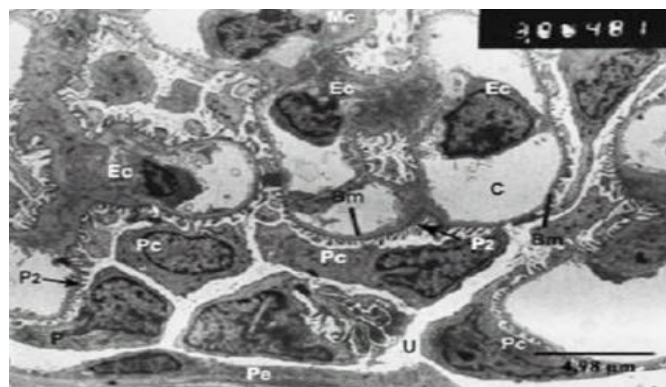


Figure 7: Electron micrograph of the renal corpuscle in the kidney of control mouse showing, the blood capillaries (C); endothelial cells (Ec); basement membrane (Bm); podocytes (Pc); secondary foot process (P2); the urinary space (U); the mesangial cells (Ms) the parietal (Pe), X 2000.

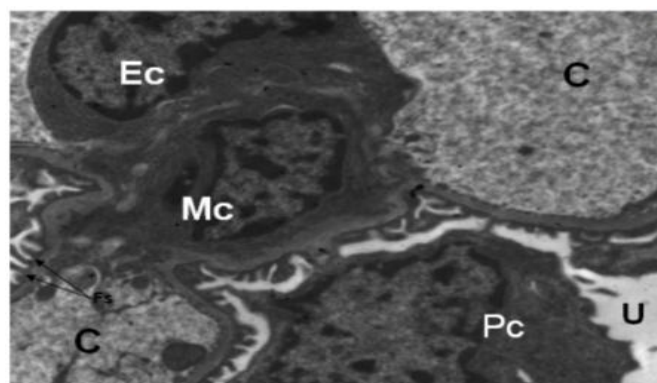


Figure 8: Electron micrograph of the renal corpuscle in the kidney of control mouse showing the Mesangial cell (Mc) interposed between the blood capillaries (C); podocytes (Pc) are suspended in the urinary space (U), heterochromatic large nucleus (N); filtration slits (fs), X4000.

The ultrastructural examination of the proximal tubule cells in the cortex of the kidney of control mice showed that they have highly polarized domains in the plasma membrane. The apical domain contains long microvilli forming a conspicuous brush border that lines the laming surface, while the basal plasma membrane domain, adjacent to the basement membrane is complex and contains numerous cytoplasmic folds project into the basal extracellular space (Fig. 9). The nuclei of these cells are roughly spherical in shape. The apical and mid regions of these cells contains rounded-shaped mitochondria, and the basal part contains dense and elongated mitochondria which are lodged in between the basolateral infoldings (Fig. 9).

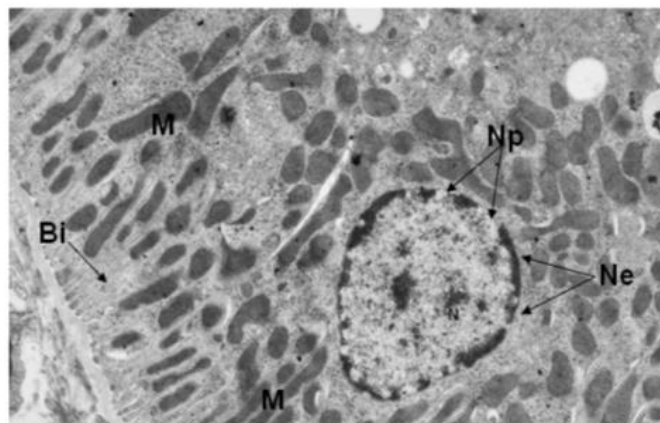


Figure 9: Electron micrograph in a proximal convoluted tubule cell in the kidney of control mouse showing, the nucleus (N) and the nuclear envelope (Ne); nuclear pores (Np); mitochondria (M); Note: the basal infolding (Bi), X 7500.

The distal convoluted tubule cells are of low columnar shaped-structure, and the luminal plasma membrane forms occasional short and blunt microvilli. These cells have rounded-shaped nuclei which are commonly located toward the apical surface of the tubular cells. The mitochondria at the apical mid regions of the tubular cells are mostly rounded in shape and small in size; while many filamentous and elongated mitochondria are located at the basal part (Fig. 10).

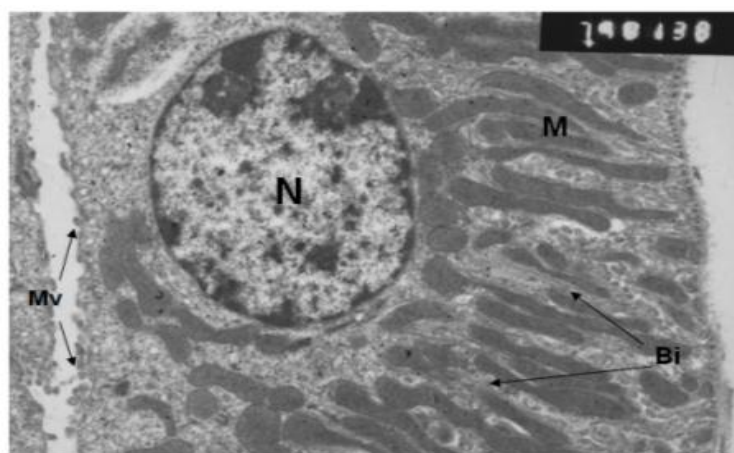


Figure 10: Electron micrograph in a distal convoluted tubule cell in the kidney of control mouse showing, apical spherical nuclei (N); Not: the mitochondria (M); short microvilli (Mv) and the basal infoldings (Bi), X 7500.

Sections in the cortical region of kidney of mice treated with 0.15 mg/kg BW cisplatin showed the the appearance of many dilated and congested blood vessels, and the malpighian corpuscles were atrophied and shrunken (Fig. 11). Both the proximal and the distal convoluted tubules displayed numerous abnormalities including damages in their morphology and cellular arrangement including loss of the tubular epithelial cells, dilatation of lumen and necrotic epithelial cells (Fig. 12). Ultrastructurally, in the renal corpuscles, mild partial collapse and the red blood cells were observed in the capillary lumen. The podocyte cells were shrunken and their cytoplasmic extensions were fragmented. The secondary foot processes or pedicels of podocytes were disordered with focal fusion (Fig. 14), and sometimes appear as marked ballooning structure. The secondary

foot processes of podocytes were longer at certain places. The basement membrane of these cells was thickened and was not uniform in its appearance (Fig. 14). The proximal convoluted tubule showed little ultrastructural alterations in both the nuclei and cytoplasm of these cells. The basement membrane became slightly thickened at certain intervals with disorganized basal infoldings. The lateral intercellular space was relatively wide. The cytoplasm contains large vacuoles, and the mitochondria attained pleomorphic shape, and exhibited irregular distribution (Fig. 15). In the distal tubule cells, few short apical microvilli were projected toward the lumen, their nuclei were irregularly outlined. The cytoplasm contains few small vacuoles, and the mitochondria were aggregated at the basal cytoplasmic part (Figs. 16, 17).

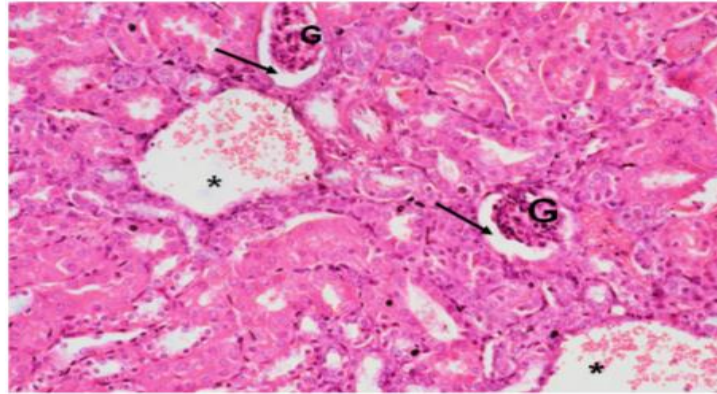


Figure 11: Light micrograph of the renal cortex in the kidney of mouse treated with 0.15 mg/kg BW cisplatin showing, atrophy of glomeruli (G); dilated urinary spaces (arrows); congested blood vessels (*), X 200.

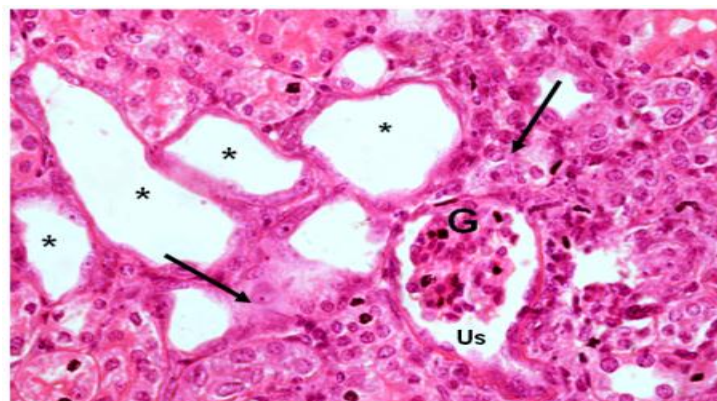


Figure 12: Light micrograph of the renal cortex in kidney of mouse treated with 0.15 mg/kg BW cisplatin showing, abnormal morphological appearance; Note: the glomerulus displays shrunken (G); dilatation in the urinary space (Us); marked tubular necrosis (-); arrows point at detached cellular debris, X 400.

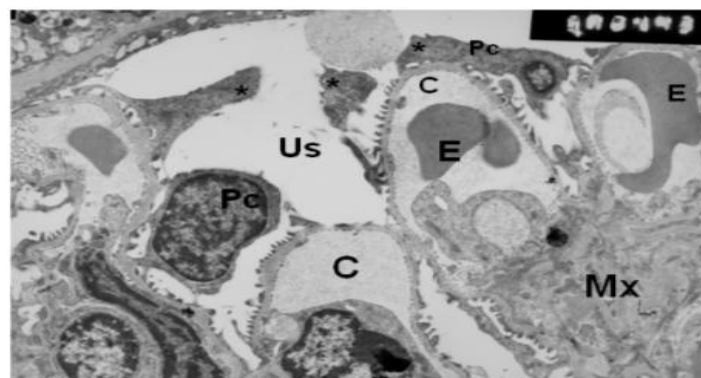


Figure 13: Electron micrograph of the renal corpuscle in the kidney of mouse treated with 0.15 mg/kg BW cisplatin showing, narrow of capillaries (C); erythrocytes (E); podocytes (Pc) exhibit shrunken and their cytoplasmic extensions are fragmented (*); Mesangial matrix (Mx), X 5000.

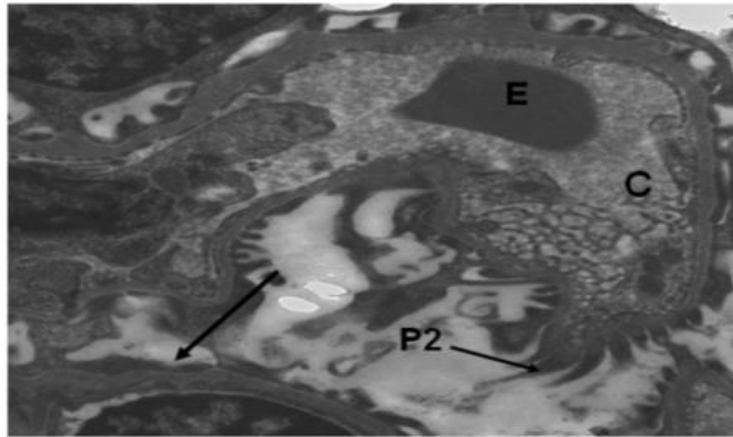


Figure 14: Electron micrograph of the renal corpuscle in the kidney of mouse treated with 0.15 mg/kg BW cisplatin showing, secondary foot processes (P2); formation a sheet of podocyte cytoplasm (arrows); wide capillary (C) contains erythrocyte (E), X 5000.

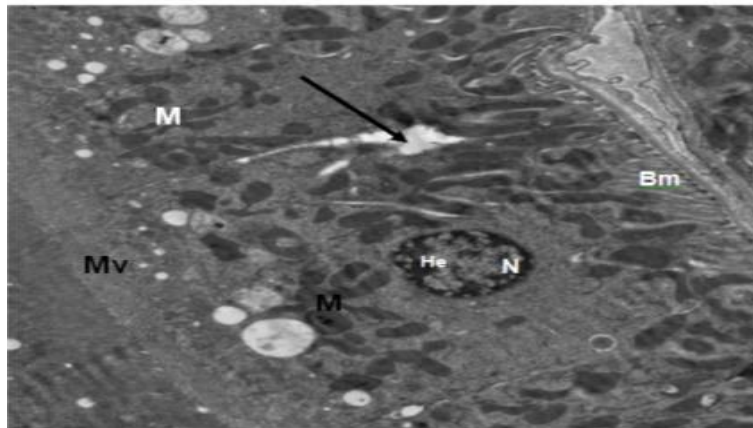


Figure 15: Electron micrograph in the proximal convoluted tubules in kidney of mouse treated with 0.15 mg/kg BW cisplatin showing, short microvillus border (Mv); pyknotic nucleus (N); Note: the pleomorphic mitochondria (M); arrow points at the intercellular space, X 2500.

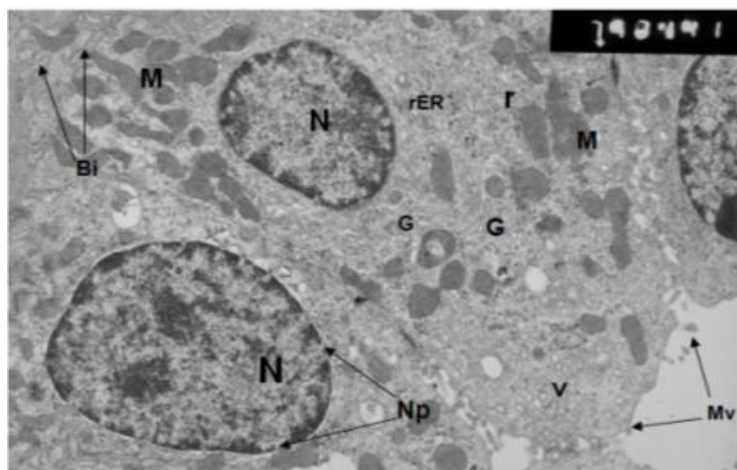


Figure 16: Electron micrograph of the distal convoluted tubule cell in the kidney of mouse treated with 0.15 mg/kg BW cisplatin showing, rupture microvilli (arrows); pleomorphic mitochondria (M); nuclei (N) with slightly irregular nuclear outline; basal infolding (Bi); Golgi apparatus (G); low rough endoplasmic reticulum (rER); pleomorphic mitochondria (M); pinocytotic vesicles (v), X 7500.

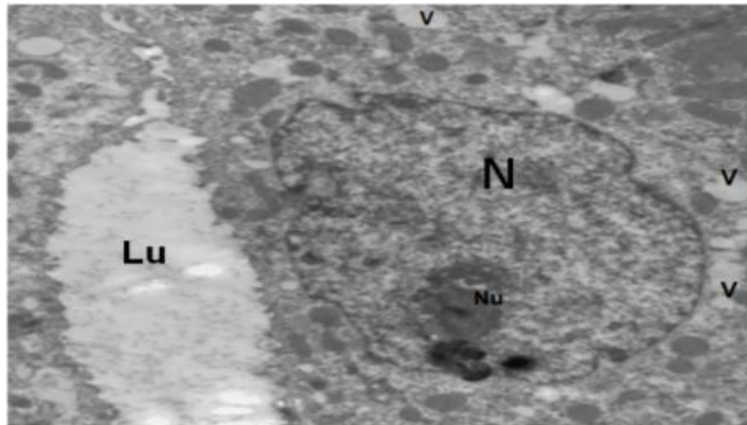


Figure 17: Electron micrograph of the distal convoluted tubule in the kidney of mouse treated with 0.15 mg/kg BW cisplatin showing, the irregular-shaped nucleus (N); Note: the presence of vacuoles (V) in the cytoplasm, X 2000.

Sections in the cortical region of kidney of mice treated with 0.3 mg/kg BW cisplatin showd marked congestion in the blood vessels, and the renal tubules had lost their regular shape, sloughing of cells and complete lysis of their cytoplasm were observed (Fig. 18). Focal inflammatory cells infiltrated were observed around the glomeruli, and most of the glomeruli exhibited shrinkage of the glomerular tuft and dilatation in the urinary spaces (Fig. 19). Further, the results revealed marked degeneration in both the proximal and distal convoluted tubules, and the presence of observable necrotic areas (Fig. 20).

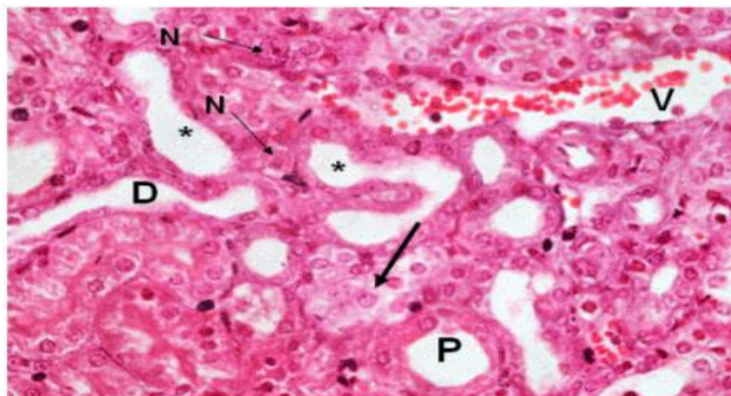


Figure 18: Light micrograph of the renal cortex in the kidney of mouse treated with 0.3 mg/kg BW cisplatin, showing the prominent distortion in the proximal (P) and the distal (D) convoluted tubules; dilatation in the lumen (*) of the tubules, loss of the epithelial lining (arrow), congested blood vessels (V), X 400.

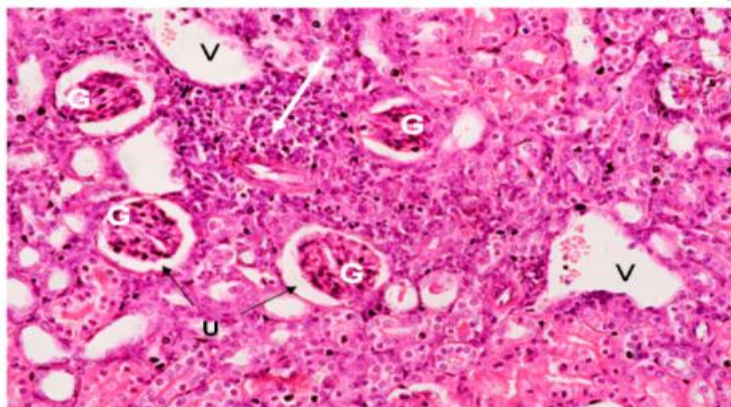


Figure 19: Light micrograph of the renal cortex in kidney of mouse treated with 0.3 mg/kg BW cisplatin, showing shrunk glomeruli (G) with densely basophilic nuclei. Also, note: dilatation of urinary space (U); focal inflammatory cells infiltration (white arrow); dilated vein (V), X 200.

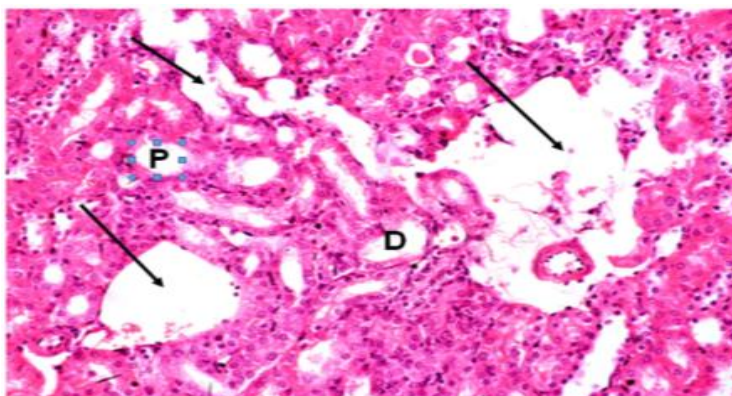


Figure 20: Light micrograph of the renal cortex in the kidney of mouse treated with 0.3 mg/kg BW cisplatin, showing disruption in the appearance of proximal (P) and distal (D) convoluted tubules; arrows point at intercellular space between the tubules, X 200.

At the ultrastructural level, the lumen of the glomerular capillaries were highly dilated and showed the presence of erythrocytes (Fig. 21). The secondary foot processes were hypertrophied and uptake ballooned-like structure (Fig. 22). The nuclei of most PCT cells were pyknotic (Figs. 23, 24). The mitochondria displayed characteristic feature of injury such as swelling, disappearance of cristae, and they were not arranged in the usual manner as in the control (Fig. 25). In addition, large vacuoles were observed in the apical part of their cytoplasm, and there was prominent increase in the primary and secondary lysosomes (Fig. 23, 25). In the distal convoluted tubule cells, the nuclei were mostly pyknotic, and the nucleoli were absent in most of them. In the cytoplasm of these cells, the mitochondria had lost their typical arrangement, where there were no focal elongated mitochondria in the basal infoldings (Fig. 26).

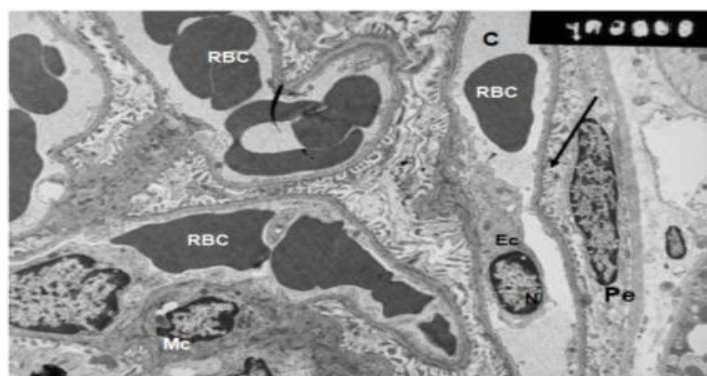


Figure 21: Electron micrograph of the renal corpuscle in the kidney of mouse treated with 0.3 mg/kg BW cisplatin, showing adhesion between parietal layer (Pe) and the visceral layer (arrow); Mesangial cell (Mc); Note: the wide congested capillaries (C), erythrocytes (RBC), X 5000.

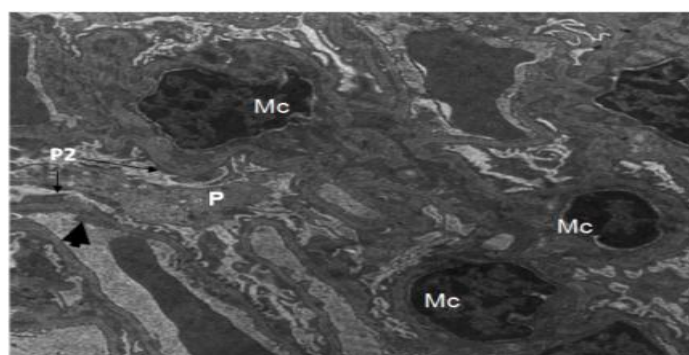


Figure 22: Electron micrograph of the renal corpuscle in the kidney of mouse treated with 0.3 mg/kg BW cisplatin, showing disorganized foot processes (P) in the podocyte; Note: the lack in the endothelial fenestrate (arrow head); Mesangial cells (Mc), X 2500.

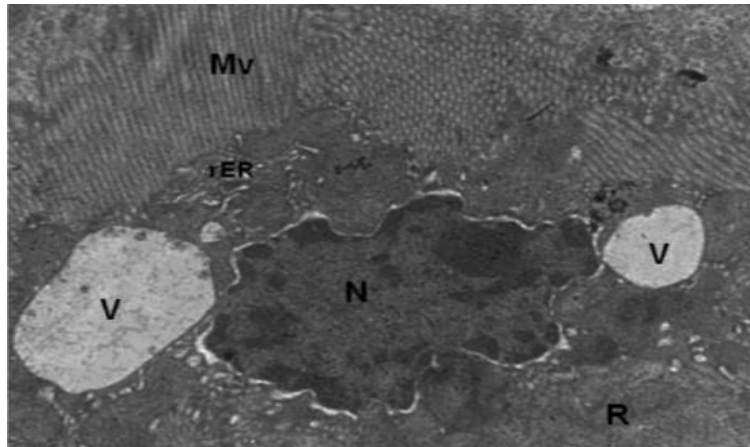


Figure 23: Electron micrograph of a proximal convoluted tubule cell in the kidney of mouse treated with 0.3 mg/kg BW cisplatin, showing a pyknotic nucleus (N), having highly folded nuclear envelop (NP); Note: the presence of large vacuoles (V) in the cytoplasm; microvilli (Mv), X 3000.

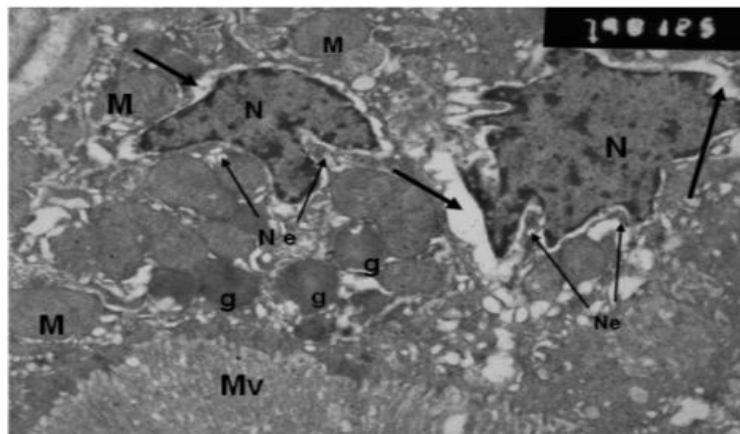


Figure 24: Electron micrograph of a proximal convoluted tubule cell in the kidney of mouse treated with 0.3 mg/kg BW cisplatin, showing two pyknotic nuclei (N) having no nucleoli; Note: different sizes and shapes of mitochondria (M); arrows point at the perinuclear spaces; many dense granules (g) in the cytoplasm; microvilli (Mv), X 7500.

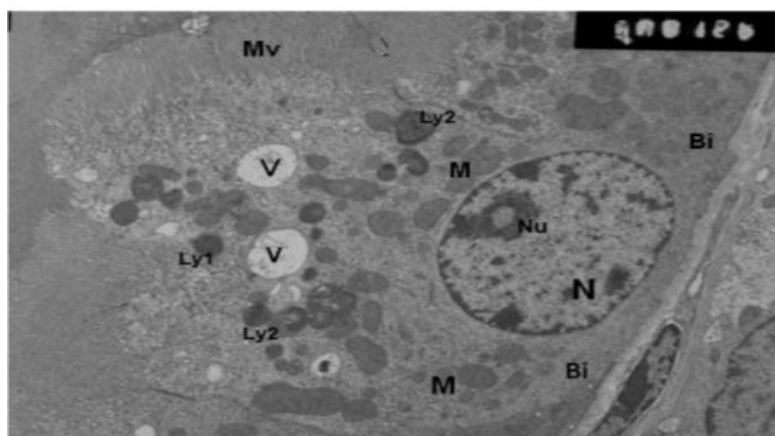


Figure 25: Electron micrograph of a proximal convoluted tubule cell in kidney of mouse treated with 0.3 mg/kg BW cisplatin, showing the disarrangement of the mitochondria (M); Note: the basally-located nucleus (N) contains compact nucleolus (Nu); primary secondary lysosomes (Lys); large vacuoles (V); microvillus (Mv), X 5000.

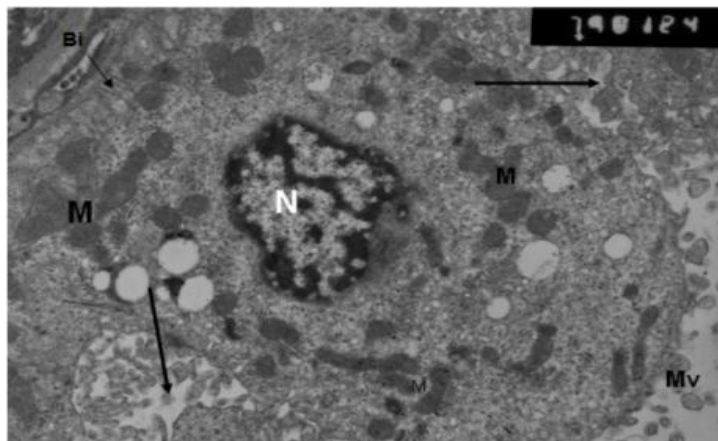


Figure 26: Electron micrograph of a distal convoluted tubule cell in the kidney of mouse treated with 0.3 mg/kg BW containing pyknotic nucleus (N); Note: the cytoplasm contains many larger vacuoles (V) and pleomorphic mitochondria (M), X 3000.

DISCUSSION

Cisplatin is a widely used and effective anticancer drug, associated with significant dose-limiting toxicities including nephrotoxicity and neurotoxicity. Depending on the dose response of cisplatin, the results revealed an increase in the mortality rate, while there is marked significant decrease in the body weight. Similarly, Dzagnidze *et al.* [21] noticed that mice injected with a single i.p dose of cisplatin (2 and 10 mg/kg BW) caused marked increase in the rate of mortality. Several investigators [9, 14, 22] reported that cisplatin had been shown to decrease the total body weight of mice and rats. This decrease in the body weight might be due to the decrease in appetite and the enhancement of the catabolic rate which is considered as the obvious side effects of the chemotherapy [23]. Atessahin *et al.* [24] explained that body weight loss might be due to the drug toxicity or the gastrointestinal toxicity and thereby reduced ingestion of food [25].

The bone marrow cells with structural chromosomal aberrations in metaphase were significantly increased in mice treated with 0.3 mg/kg BW cisplatin. These chromosomal aberrations were mainly performed in the formation of chromatid breakages (deletion, gap, break and fragment). Febrer *et al.* [26] explained that the chromosomal damage after G1 stage of the cell cycle causes chromatid damages and chromatid breakage. Ito and Matsumoto [27] explained that the centromeric attenuation of chromosomes is indication for splitting of the centromere without mitosis may be an early stage of endomitosis, in which case it gives rise to polyploidy. This increase in centromerically chromosomal attenuation indicated the effect of cisplatin on the spindle apparatus and the polyploidy [10, 28].

The current results indicated histological and ultrastructural changes of the cortical region of kidney of mice treated with the two different doses of cisplatin. These changes include severe atrophy in the glomeruli; rupture of Bowman's capsule and dilatation in the urinary space. These results are confirmed by the report documented by Ravindra *et al.* [29] who demonstrated that cisplatin could induce acute renal necrosis with marked congestion of the glomeruli and glomerular atrophy. Karimi *et al.* [30] found that 3 mg/kg cisplatin for 5 days showed severe tubular necrosis among kidney sections of rats. In addition, there was progressive tubular damage in both proximal and the distal convoluted tubules, manifested in fragmented microvilli, increased frequency of pyknotic nuclei, cytoplasmic vacuolization, increased lysosomes and changes in the mitochondrial structure and arrangement. Behling *et al.* [31] suggested that cisplatin acts mostly on the proximal convoluted tubules. Shalaby *et al.* [32] found degenerative changes in the proximal convoluted tubules in the kidney of male albino mice administered with cisplatin over 21 days. Kim *et al.* [33] had reported that cisplatin caused nephrotoxicity which was evidenced by significant loss of brush-border microvilli which is supposed to be responsible for reducing the area for active glucose reabsorption [34]. The mesangium cells were characterized by highly electron dense mesangial matrix. These data are in close correlation with those reported by Kohn *et al.* [35] who studied the nephrotoxic effect of cisplatin on kidney glomerular components in guinea pigs. Moreover, the present results revealed that the mesangial cells appeared irregular with bizarre shaped nuclei and dense matrices. It is conceivable that even a minor reduction in the mesangial

cell area could affect the filtering surface of the glomeruli and explained the decrease in the glomerular filtration [36].

Further, the current results revealed marked focal loss in the brush border, pyknotic nuclei, chromatin condensation, swelling of the mitochondria with regression of the mitochondrial crista, in addition to the increased number of lysosomes. However, there were much less distal convoluted tubules changes, including minimal microvilli, pyknotic nuclei and organelles disorganization. Abdelmeguid *et al.* [22] revealed great similarities to a certain extent with our results, where cisplatin resulted in focal and severe tubular changes in PCT and DCT cells, in male albino mice.

CONCLUSION

The results of the current study suggest that cisplatin could induce nephrotoxicity, causing DNA damage, appearance of chromosomal aberrations, and ultrastructural alterations in all parts of the renal tubules and the renal corpuscles. This indicates that other new chemotherapeutic drugs should be discovered in order to decrease their possible toxic side effects on the human health.

REFERENCES

- [1] Chandrasekar MJN, Bommu P, Nanjan MJ and Suresh B. *J Phar Bio* 2006;44(2): 100 – 106.
- [2] Holland JF, Bast RC, Morton DL, Frei E, Kufe DW and Weichselbaum RR. *Chemotherapeutic agents*. In *Cancer Medicine*. 4th ed. (Williams & Wilkins, Baltimore, MD) 1997;pp. 907–1045.
- [3] Shah N and Dizon DS. *Future Oncol* 2009;5:33–42.
- [4] Zhang J, Wang L, Xing Z, Liu D, Sun J, Li X and Zhang Y. *Anticancer Agents Med Chem* 2010;10: 272–282.
- [5] Mansour HH, Hafez FH and Fahmy NM. *J Biochem Mol Biol* 2006;39: 656 - 661.
- [6] Miller RP, Tadagavadi RK, Ramesh, et al. *Toxins (Basel)* 2010;2: 2490 – 2518.
- [7] Ajith TA, Usha S and Nivitha V. *Clin Chim Acta* 2007;375: 82 – 86.
- [8] Ali BH and Al-Moundhri MS. *Food Chem Toxicol* 2006; 44: 1173-1183.
- [9] Saad AA, Youssef MI, El-Shennawy LK. *J Food and Chem Toxicol* 2009;47: 1499–1506.
- [10] Nersesyan A, Perrone E, Roggeri, P and Bolognesi, C. *Chemother* 2003 49: 132- 137.
- [11] Yoshida J, Kosaka H, Tomioka K and Kumagai S. *J Occup Health* 2006;48: 517 - 522.
- [12] Florea AM and Büsselberg D. *Cancers* 2011; 3: 1351 - 1371.
- [13] Sahu BD, Reddy KKR, Putcha UK, et al. *Food Chem Toxicol* 2011;49: 3090–3097.
- [14] Domitrovic R, Potocnjak I, Crnc̃ević-Orlic Z, Škoda M. *Food Chem Toxicol* 2014;66: 321– 328.
- [15] Park MS, Maryely DL and Devarajan PJ. *Am Soc Nephrol* 2002;13: 858 – 865.
- [16] Custódio JB, Cardoso CM, Santos MS, Almeida LM, Vicente JA, Fernandes MA. *Toxicol* 2009;259: 18 – 24.
- [17] Abdelwahab HMF, Hassanin NIY, Ahmed EM and Abd El-Monem AR. *Aust J Basic Appl Sci* 2011;5 (10): 231 - 238.
- [18] Preston RJ, Dean BJ, Galloway S, Holden H, McFree AF and Shelby M. *Mutat Res* 1987;189: 157– 165.
- [19] Bancroft JD and Gamble M. *Theory and Practice of Histological Techniques*. 5th (Ed.) Churchill Livingstone, London, 2002;p. 153.
- [20] Hayat MA. *Principles and techniques of electron microscopy: Biological applications*. 4th ed. Cambridge: Cambridge University Press, 2000; pp 24 - 96.
- [21] Dzagnidze A, et al. *The J Neurosci* 2007; 27(35): 9451 – 9457.
- [22] Abdelmeguid NE, Chmairie HN and Abou Zeinab NS. *Pak J Nutr* 2010; 9 (7): 624-636.
- [23] Hassan I, Chibber S, Naseem I. *Food Chem Toxicol* 2010;48: 2052-2058.
- [24] Atessahin A, Yilmaz S, Karahan I, Ceribasi, AO and Karaoglu A. *Toxicol* 2005;212: 116 – 123.
- [25] Tikoo K, Bhatt DK, Gaikawad, AB, Sharma V and Kabra, DG. *FEBS Lett* 2007;581: 2027–2035.
- [26] Febrer, E, Mestres, M, Caballín, M. R, Barrios, L, Ribas, M, Gutiérrez-Enríquez, S, Alonso, C, Ramón, y, Cajal T, Francesc BJ. *DNA Repair (Amst)* 2008;7 : 1907 - 1911.
- [27] Ito D and Matsumoto T. *Adv Exp Med Biol* 2010;676: 15 - 26.
- [28] Misra S and Choudhury, RC. *J Chemother* 2006;18: 182 - 187.
- [29] Ravindra P, Bhiwgade DA, Kulkarni S, Rataboli V and Dhumem Y. *J Cell Anim Biol* 2010; 4(7): 108 - 111.
- [30] Karimi, G, Ramezani M. and Tahoonian, Z. *Evid Based Complement Alternat Med* 2005;2: 383 - 386.



- [31] Behling EB, et al. Pharmacol Rep 2006;58: 526 - 532.
- [32] Shalaby T, Ghanem AM and Ramadan HS. Romanian J Biophys 2006;4: 229 - 241.
- [33] Kim YK, Byun, HS, Kim YH, Woo JS and Lee SH. Toxicol Appl Pharmacol 130: 19-26.
- [34] Devipriya S. and Shamala D. J. Pharmacol 1995;3: 422-426
- [35] Kohn S, Fradis M, Ben-David J, Zidan J and Robinson E. Ultrastructural Pathol 2002;26: 371-382.
- [36] Rodriguez-Barbero A, L'Azou B, Cambar J and Lopez-Novoa, JM. Cell Biol Toxicol 2000;16: 145-53.